

Evolution from 4f-electron antiferromagnetic to ferromagnetic order in the CeCu(Ge_{1-x}Sn_x) alloy series (0 ≤ x ≤ 1)

A. Altayeb,^{1,2} B. M. Sondezi,² M. B. Tchoula Tchokonté,^{1,a} A. M. Strydom,² T. B. Doyle,^{3,4} and D. Kaczorowski⁵

¹Department of Physics, University of the Western Cape, Private Bag X 17, Bellville 7535, South Africa

²Highly Correlated Matter Research Group, Department of Physics, University of Johannesburg, P.O. Box 524, Auckland Park 2006, South Africa

³Materials Research Group, iThemba LABS, P.O. Box 722, Somerset West 7129, South Africa

⁴School of Chemistry and Physics, University of KwaZulu-Natal, Durban 4001, South Africa

⁵Institute of Low Temperature and Structure Research, Polish Academy of Sciences, P.O. Box 1410, 50 - 950 Wrocław, Poland

(Presented 1 November 2016; received 22 September 2016; accepted 16 November 2016; published online 16 February 2017)

We report the evolution from ferromagnetic (FM) to antiferromagnetic (AFM) state in CeCu(Ge_{1-x}Sn_x) investigated by means of magnetic and heat capacity measurements. X-ray diffraction studies for all compositions indicate the ZrBeSi - type hexagonal crystal structure with space group $P6_3/mmc$ (No. 194). The magnetic susceptibility, $\chi(T)$ at high temperature follows the Curie - Weiss relation with an effective magnetic moment close to the value of $2.54 \mu_B$ expected for free Ce³⁺ - ion. At low temperatures, $\chi(T)$ data indicate AFM transition for alloys in the concentration range $0.7 \leq x \leq 1$ and FM for $x \leq 0.6$. The magnetization, $M(\mu_0H)$ of samples exhibiting AFM behaviour shows metamagnetic transition at low magnetic fields with some irreversibility in the process of increasing and decreasing magnetic field. In turn, $M(\mu_0H)$ of samples exhibiting FM behaviour shows saturation in high magnetic fields. Heat capacity, $C_p(T)$ data confirm the AFM and FM transitions observed in magnetic measurements. An additional anomaly below T_C and T_N is observed in $C_p(T)/T$, which likely arises from spin reorientation or rearrangement in FM or AFM structure. Below in FM region, $C_p(T)$ can be well described assuming spin-waves excitations with an energy gap Δ_C . © 2017 Author(s). All article content, except where otherwise noted, is licensed under a Creative Commons Attribution (CC BY) license (<http://creativecommons.org/licenses/by/4.0/>). [<http://dx.doi.org/10.1063/1.4977019>]

I. INTRODUCTION

The compounds RTX (R = f - electron, T = d - electron, X = p - electron) crystallize in different crystal structures and order magnetically in a wide temperature range.¹ Large amount of experimental research was devoted to the compounds CeCuGe^{2,3} and CeCuSn^{4,5} probing their magnetic and electronic properties. Both compounds were found to crystallize in structures derived from the hexagonal AlB₂ - type with Ce atoms located on the Al site.

The compound CeCuGe has been reported to order ferromagnetically at $T_C = 10$ K.^{4,6} In the paramagnetic state it exhibits Curie-Weiss behavior with an effective magnetic moment (μ_{eff}) per Ce of $2.50 \mu_B$ that is close to the value of 2.54 expected for free Ce ion.³ The resistivity data of this compound follows the T^2 - power law in the temperature range 10 - 30 K, consistent with the appearance of spin fluctuations above T_C .³ In the ordered state, the resistivity behavior can

^aCorresponding author: mtchokonte@uwc.ac.za

interpreted in terms of scattering conduction electrons on magnons. The heat capacity of CeCuGe shows a Schottky - type anomaly around 68 K associated with crystalline electric field (CEF) effects.⁶

The CeCuSn compound has been reported to order below 8.6 K with a complex AFM - type structure.⁴ In the ordered state, the heat capacity exhibits a maximum near 7.4 K, signalling a rearrangement of the AFM structure.⁷ Two structural modifications of CeCuSn were synthesized by Sebastian *et al.*⁸ The high-temperature β - CeCuSn phase crystallizes with the hexagonal NdPtSb-type structure, while the low-temperature α - CeCuSn phase adopts the hexagonal structure of the ZrBeSi-type.

In view of the different magnetic states in CeCuGe and CeCuSn, we found it interesting to investigate a solid solution of the two compounds CeCu(Ge_{1-x}Sn_x). Here, we report the results of magnetic and heat capacity measurements of this alloy series.

II. EXPERIMENTAL DETAILS

Polycrystalline samples of CeCu(Ge_{1-x}Sn_x) were prepared by arc - melting stoichiometric amounts of the elements (purities in at %) Ce (99.98), Cu (99.995) Ge and Sn (99.999) under ultra - high purity argon atmosphere. The samples were overturned and remelted three times to promote homogeneity. The weight losses after final melting were always less than 1 wt.%. Subsequently, the sample ingots were wrapped in tantalum foil, encapsulated in evacuated quartz tubes, and annealed at 850^oC for two weeks.

The products were checked by powder X - ray diffraction using a Bruker D8 ADVANCE diffractometer with CuK α radiation ($\lambda = 1.5406\text{\AA}$). The X - ray diffraction spectra were analyzed using the cell and intensity least - squares (CAILS) - Pawley refinement method from TOPAS ACADEMIC.

Temperature- and magnetic field-dependent properties of the prepared alloys were measured using commercial equipment, namely a Quantum Design Physical Property Measurement System (PPMS) and a Magnetic Property Measurement System (MPMS).

III. RESULTS AND DISCUSSION

A. X - ray diffraction

X - ray diffraction obtained for the two end compounds as well as two other compositions in the series together with the CAILS refinement fits to the data, are shown in Fig. 1. The space group setting used in the CAILS - Pawley refinement was $P6_3/mmc$ hexagonal ZrBeSi - type structure. The results of the refinements are shown by black solid lines through the measured data and the Sn content (x) dependence of the lattice parameters (a and c) and unit cell volume (V) are shown in the insets of Fig. 1. It is observed that V and a increase linearly with x . The linear increase in V is consistent with Vegard's law which suggests the stability of the Ce valence across the series as well as no change in the number of conduction electrons, which ensures metallic bonding of the alloy system.

B. Magnetic susceptibility and magnetization

The inverse magnetic susceptibility, $\chi^{-1}(T)$ of the CeCu(Ge_{1-x}Sn_x) alloys, measured in a field of 0.1 T in the temperature range $1.7 \leq T \leq 400$ K, are shown in Fig. 2. At temperatures above 100 K, $\chi^{-1}(T)$ exhibits Curie - Weiss (CW) behaviour:

$$\chi^{-1}(T) = \frac{3k_B(T - \theta_p)}{N_A \mu_{eff}^2}, \quad (1)$$

where all the parameters have their usual meaning. Least squares fits (LSQ) against the experimental data are shown as solid lines in Fig. 2. Parameters obtained from these fits are gathered in Table I. At lower temperature, $\chi^{-1}(T)$ data deviate from CW linear behaviour and this may be attributed to the onset of magnetic ordering or CEF effect. The obtained μ_{eff} values are reasonably close to that predicted within a Russel - Saunders coupling scenario for the trivalent Ce - ion ($2.54 \mu_B$). This finding indicates fairly stable $4f$ electronic state of the cerium atoms. For

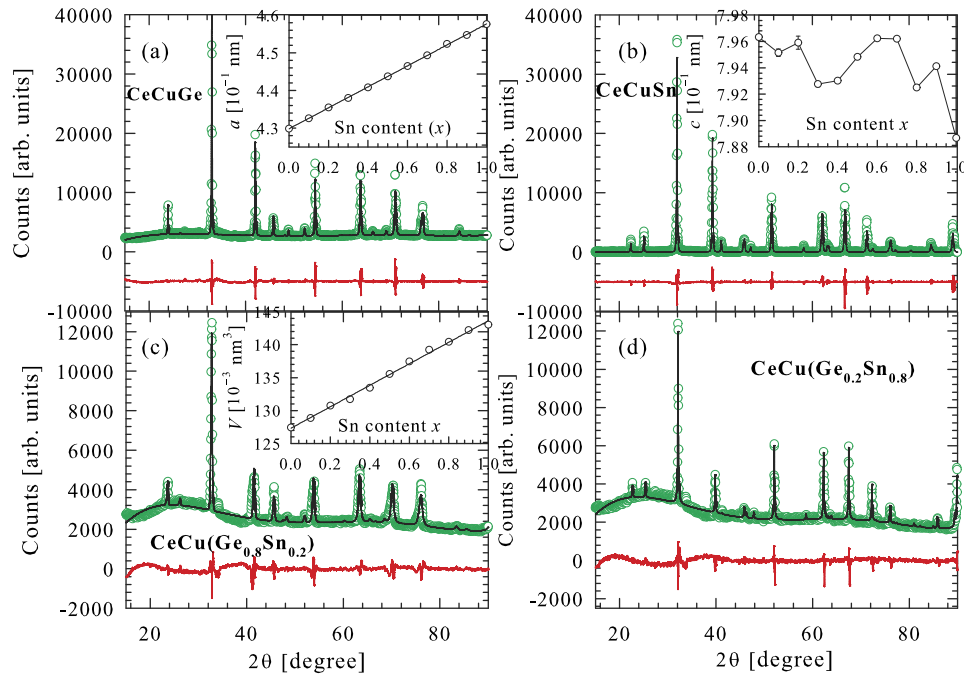


FIG. 1. CAILS analysed patterns of selected compositions in $\text{CeCu}(\text{Ge}_{1-x}\text{Sn}_x)$. The observed data are shown by green symbols and the solid black lines through the data represent the result of the CAILS refinement. The lower red curves are the difference curves between the experimental data and the calculated curves. The insets show the Sn content x dependence of the lattice parameters a (a) and c (b) and the unit cell volume V (c).

all compositions, the Weiss temperature was found negative. The negative values of θ_p for FM compositions indicate that regardless the FM ordering, also these systems are dominated by AFM exchange interactions. The low temperatures, $\chi(T)$ data measured in field of 0.1 T are shown in Fig. 3 for selected compositions in the AFM and FM region. For compositions in the range $0.7 \leq x \leq 1$, $\chi(T)$ data show a kink associated to PM - AFM transition at T_N as indicated by arrows in Fig. 3a. Below T_N , an abrupt rise of $\chi(T)$ data is observed which may be associated to coexistence of AFM and FM exchange interactions or canting of the AFM structure. As shown in Figs. 3b–3d, $\chi(T)$ data of the compositions with $x \leq 0.6$ exhibits a FM - like behaviour. The PM - FM transition around T_C was estimated from the minimum value of $d\chi(T)/dT$ curves (right axis) for each composition as indicated by arrows in the figures. The estimated values of T_N and T_C from $\chi(T)$ data are listed in Table I. The obtained values of T_N and T_C for the two end compounds are in good agreement with previously reported values of $T_C = 10 \text{ K}$ ^{4,6} for CeCuGe and $T_N = 8.6 \text{ K}$ for CeCuSn .⁷

The field-dependent magnetization was measured in fields up to 5 T at $T = 1.7 \text{ K}$. $M(\mu_0H)$ for compositions with $x \geq 0.7$ (inset Fig. 3a), initially increases linearly up to a critical field, then deviate from linearity at high field. This deviation is associated to field - induced magnetic transition occurring in these alloys, at the critical field. Small hysteresis was observed for these compositions in the process of increasing and decreasing field. As shown in the insets of Figs. 3b–3d, $M(\mu_0H)$ of compositions with $0 \leq x \leq 0.6$ exhibits a FM - like behaviour characterized by an abrupt rise of $M(\mu_0H)$ upon application of weak magnetic field, followed by a tendency towards saturation in high fields. For all compositions, the magnetization measured in 5 T at 1.7 K is less than $1.1 \mu_B$, which is approximately half the theoretical value for free Ce^{3+} ion ($g_J J = 2.14 \mu_B$). The difference can be attributed to the CEF effects.

C. Heat capacity

The $4f$ - electron contribution to the specific heat, $C_{4f}(T)$, of selected compositions is presented in Fig. 4. The data was obtained by subtracting from the measured $C_p(T)$ curves the phonon contribution

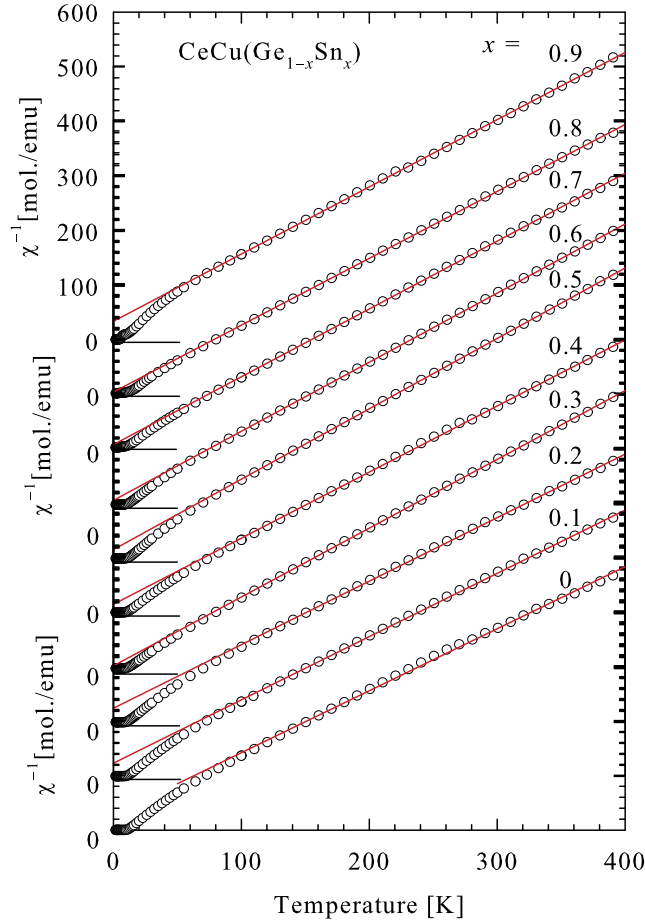


FIG. 2. $\chi^{-1}(T)$ data of $\text{CeCu}(\text{Ge}_{1-x}\text{Sn}_x)$ alloy series with the Curie - Weiss fits (Eq. 1, red solid line) according to the experimental data above 100 K.

resulting from the fits of the conventional equation for the specific heat of a metal at temperature well above T_C and T_N : $C_p(T)/T = \gamma^{\text{conv}} + \beta T^2$ (see insets of Fig. 5). The magnetic phase transitions in these compositions manifest themselves as clear maxima in the $C_p(T)/T$ curves (see insets of Fig. 4). The so-derived values of T_C and T_N , listed in Table I, are close to those obtained from the $\chi(T)$ data. A second anomaly below T_C and T_N at $T_{i1} = 4.6$ K and 3.2 for compositions with $x = 0.4$ and 0.8

TABLE I. Magnetic susceptibility parameters of the alloys series $\text{CeCu}(\text{Ge}_{1-x}\text{Sn}_x)$.

Sn content x	$\mu_{\text{eff}}[\mu_B]$	$-\theta_p[\text{K}]$	$T_C^\chi(T_C^{C_p})[\text{K}]$	$T_N^\chi(T_N^{C_p})[\text{K}]$
1	2.629(4)	18.9(8)		8.6
0.9	2.307(2)	29.3(6)		10
0.8	2.319(2)	4.3(8)		9.5(7.3)
0.7	2.287(2)	6.2(5)		9
0.6	2.444(1)	6.3(4)	10(9.2)	
0.5	2.201(1)	12.7(3)	10	
0.4	2.346(3)	12(1)	9.5(8.7)	
0.3	2.253(1)	4.0(4)	9.7	
0.2	2.441(3)	22(1)	9.7(9)	
0.1	2.450(4)	21(1)	10	
0	2.500(3)	25(2)	11	

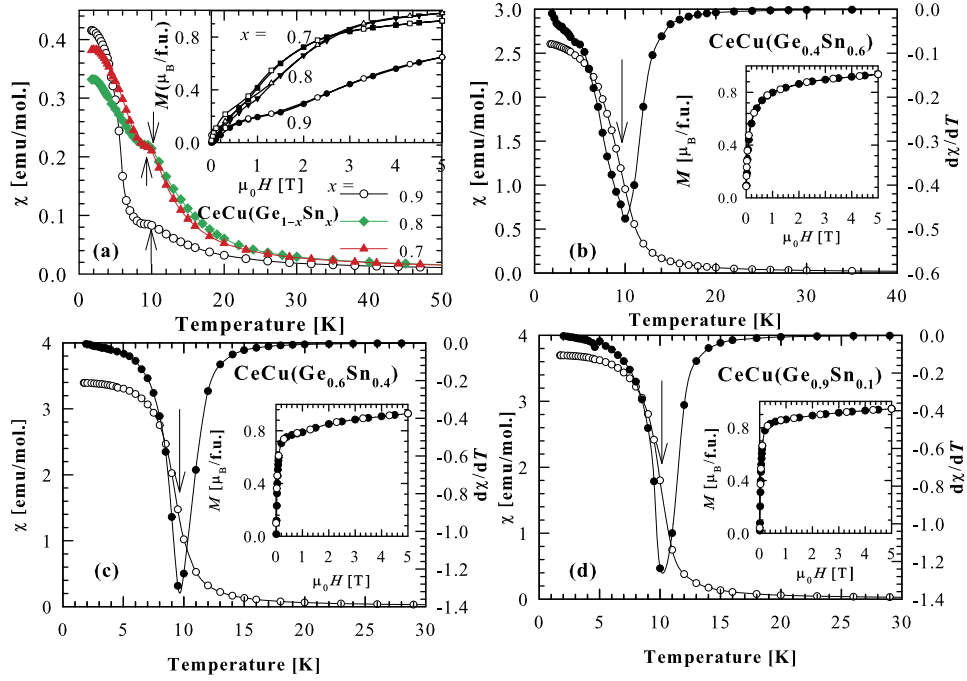


FIG. 3. Low temperature $\chi(T)$ data of selected compositions of $\text{CeCu}(\text{Ge}_{1-x}\text{Sn}_x)$ alloy series in the AFM region (a) and in the FM region (b), (c) and (d). The insets show the $M(\mu_0H)$ data measured in increasing (closed symbols) and decreasing (open symbols) field. The arrows in (a) indicate the AFM transition temperature T_N taken at the kink (a) while the arrows in (b), (c) and (d) indicate the FM transition temperature T_C taken at the minimum value of $d\chi/dT$.

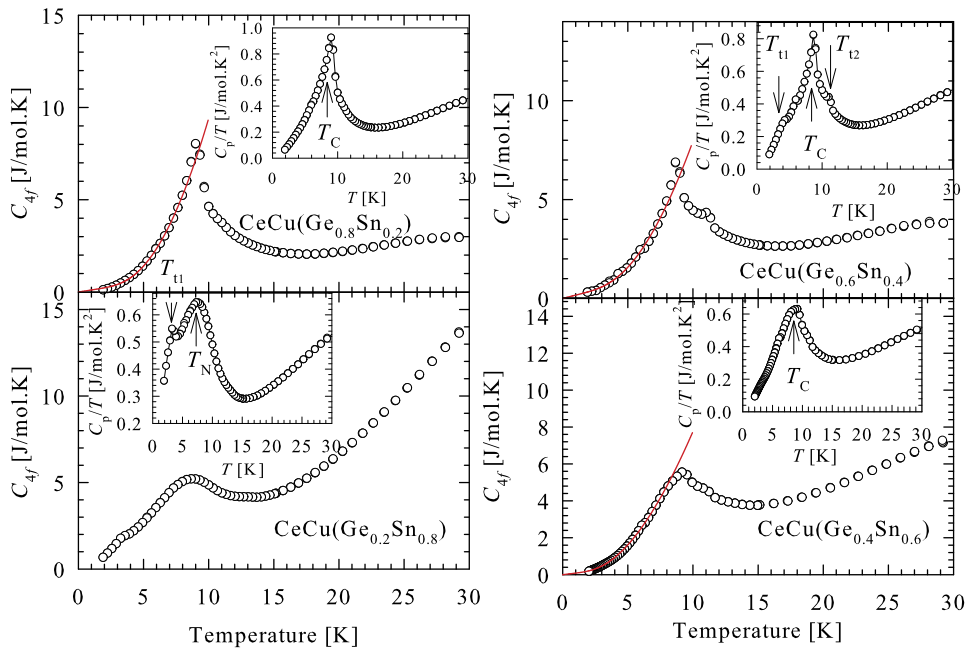


FIG. 4. The low temperature of the $4f$ -electron specific heat, $C_{4f}(T)$ of selected compositions in the FM and AFM region. The red solid curves through the data points are LSQ fits of the spin-waves spectrum expression (Eq. 2). The insets show $C_p(T)/T$ plots with the arrows indicating the magnetic phase transition temperature.

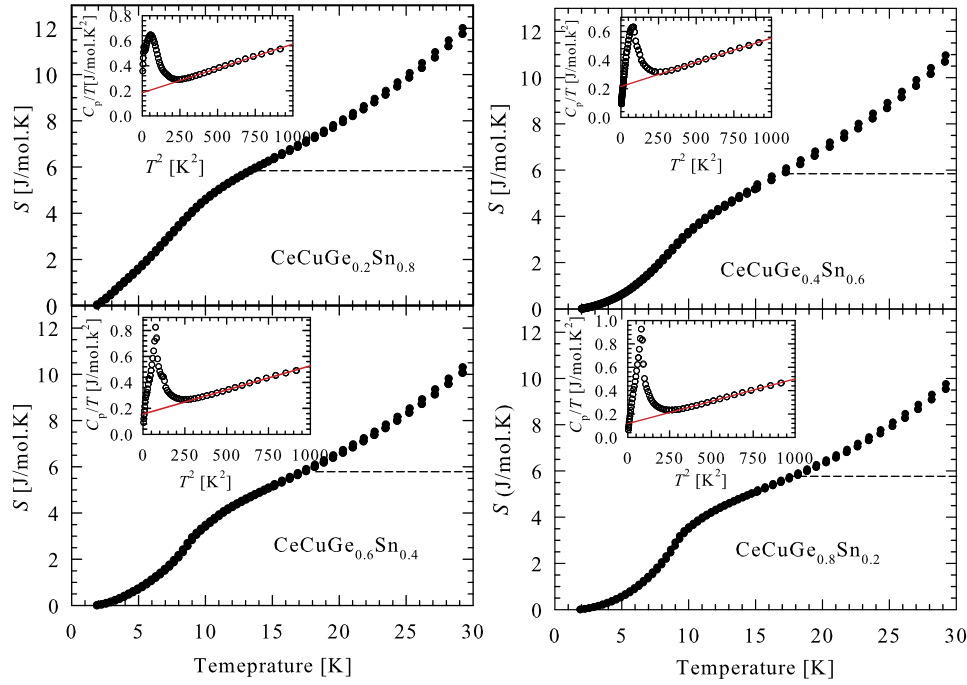


FIG. 5. The total entropy, $S(T)$ with the insets showing the plot of C_p/T vs. T^2 and the red solid lines showing the fits of the conventional equation for the specific heat of a metal well above T_C and T_N (see text).

TABLE II. Heat capacity data of the alloys series $\text{CeCu}(\text{Ge}_{1-x}\text{Sn}_x)$.

Sn content x	γ [J/mol.K ²]	A [J/mol.K ^{5/2}]	Δ_C [K]
0.2	0.112(9)	0.91(6)	12.4(6)
0.4	0.17(2)	0.59(8)	11(1)
0.6	0.086(3)	0.450(7)	7.2(2)

respectively is observed. These anomalies may be associated with spin reorientation or rearrangement of the FM or AFM structure also observed previously in CeCuSn .⁷ In the case of $x = 0.4$, another anomaly is observed above T_C at $T_{I2} = 11.3$ K. Below T_C , $C_{4f}(T)$ data can be described assuming magnon excitations, with an energy gap Δ_C in the FM spin - waves spectrum (solid red curves in Fig. 4). Applying the formula

$$C_{sw}(T) = \gamma T + AT^{3/2} \exp\left(-\frac{\Delta_C}{T}\right), \quad (2)$$

where γ is the Sommerfeld coefficient and A a constant, one obtained by LSQ fitting the parameters gathered in Table II. The values of Δ_C and A obtained for $x = 0.2$ are of the same order of magnitude as those reported before for CeCuGe .⁶ As can be inferred from Table II, Δ_C and A decrease with increasing the Sn content x .

Fig. 5 displays the entropy $S(T)$ calculated from the $C_p(T)$ data as $S(T) = \int_0^T \left[\frac{C_p(T')}{T'} \right] dT'$. For all the measured compositions, $S(T)$ reaches a value of $R \ln 2$ expected for doublet ground state somewhat above the respective transition temperature (Black dashed lines Fig. 5).

IV. CONCLUSION

Magnetic and heat capacity measurements of $\text{CeCu}(\text{Ge}_{1-x}\text{Sn}_x)$ indicate that FM ordering extends up to 60% Sn substitution. For compositions with $x \geq 0.7$, AFM ordering is observed with a kind of

spin - reorientation in the ordered region. $C_p(T)$ data below T_C can be well described assuming spin - waves excitations.

ACKNOWLEDGMENTS

Support is acknowledged from the SA-NRF (81296). The Research Development of UWC for financial support. AMS and BMS thanks the SA-NRF (93549), the SA-Thuthuka (99231) and the Faculty of Science and URC of UJ for financial assistance.

¹ S. Gupta and K. G. Suresh, *J. Magn. Magn. Mater.* **391**, 151 (2015).

² A. Szytula and J. Leciejewicz, *Handbook of Crystal Structures and Magnetic Properties of Rare Earth Intermetallics* (CRC Press, Boca Raton, FL, 1994), p. 83.

³ Y. Oner, O. Kamer, J. H. Ross, Jr., C. S. Lue, and Y. K. Kuo, *Solid State Commun.* **136**, 533 (2005).

⁴ F. Yang, J. P. Kuang, J. Li, E. Brück, H. Nakotte, F. R. Boer, X. Wu, Z. Li, and Y. Wang, *J. Appl. Phys.* **69**, 4705 (1991).

⁵ S. Chang, Y. Janssen, V. O. Garlea, J. Zarestky, H. Nakotte, and R. J. McQueeney, *J. Appl. Phys.* **97**, 10A913-1 (2005).

⁶ B. M. Sondezi, Physical properties of ferromagnetic CeTX compounds, T = Cu, Au; X = Si, Ge, PhD thesis, University of Johannesburg (2014).

⁷ H. Nakotte, E. Brück, K. Prokes, J. H. V. Brabers, F. R. de Boer, L. Havela, K. H. J. Buschow, and H. Fu-ming, *J. Alloy. Compd.* **207-208**, 245 (1994).

⁸ C. P. Sebastian, S. Rayaprol, R.-D. Hoffmann, U. Ch. Rodewald, T. Pape, and R. Potteden, [arXiv:cond-mat/0612225](https://arxiv.org/abs/cond-mat/0612225).